

## Zero- and low-field spin relaxation studied by positive muons

R. S. Hayano, Y. J. Uemura, J. Imazato, N. Nishida, T. Yamazaki, and R. Kubo

*Department of Physics, University of Tokyo, Bunkyo-ku, Tokyo, Japan**and TRIUMF, Vancouver, Canada*

(Received 27 February 1979)

Zero- and low-field spin-relaxation functions have been studied for the first time by using positive muons, and results are compared with the stochastic theory of low-field relaxation formulated by Kubo and Toyabe. The dipolar broadening of the zero-field relaxation has been studied in detail. In  $ZrH_2$ , the zero-field relaxation function of  $\mu^+$  has been found to decay  $(5)^{1/2}$  times faster than the high-field relaxation function, which is explained in terms of the contribution of the nonsecular part of the dipolar interaction. Advantages of the zero-field method over the conventional muon-spin rotation method in practical applications, especially for studies of the  $\mu^+$  diffusion/trapping, are discussed.

## I. INTRODUCTION

In this paper, we report on the study of zero- and low-field spin-relaxation functions using positive muon ( $\mu^+$ ). Theoretically, the zero- and low-field relaxation functions, where random fields exceed an external field, were formulated in a general stochastic treatment of Kubo and Toyabe.<sup>1</sup> Experimentally, however, no work has been done on this subject simply because NMR techniques are not applicable to very low resonance frequencies. On the other hand, using  $\mu^+$ , we can easily observe relaxation functions at any external field;  $\mu^+$  is a radiative probe which emits a positron preferentially along its spin direction, so that the relaxation function can be observed from the time variation of the  $\mu - e$  decay asymmetry without rf field, though the time window is limited by its lifetime  $\tau_\mu = 2.20 \mu\text{sec}$ . Furthermore, it is a pure magnetic probe (since its spin is  $\frac{1}{2}$ ) with a large gyromagnetic ratio  $\gamma_\mu = 2\pi \times 13.554 \times 10^3 / \text{Oe/sec}$ .

Usually, the relaxation of the  $\mu^+$  spin is studied via the muon spin-rotation method by applying a transverse magnetic field to measure the positron time spectrum

$$N_x(\theta, t) = N_0 \exp(-t/\tau_\mu) \times [1 + AG_x(t) \cos(\theta - \omega_\mu t)] \quad (1)$$

where  $G_x(t)$ , the envelope of the damping of the Larmor precession, represents the transverse relaxation function. Another way of measurement is called the "longitudinal-field" method where we simply apply a longitudinal external field (including zero field) to the  $\mu^+$  spin and observe the longitudinal relaxation function  $G_z(t)$  in the expression

$$N_z(\theta, t) = N_0 \exp(-t/\tau_\mu) \times [1 + AG_z(t) \cos\theta] \quad (2)$$

We employ this method at TRIUMF, since, as will be shown later, this method is superior to the transverse-field method in many respects.

After a brief description of the experimental procedure in Sec. II, we will discuss the following topics. In Sec. III, the first observation of the zero- and low-field relaxation function in MnSi is reported. The observed function was found to be a typical example of the static limit of the Kubo-Toyabe relaxation function, indicating that the relaxation is caused by static nuclear dipolar fields. In Sec. IV, the effect of muon diffusion is taken into account and general expressions for  $G_z(t)$  and  $G_x(t)$  are derived. It is shown that even an extremely slow muon diffusion can be detected by using the zero-field relaxation function whereas the conventional high-field transverse relaxation function is insensitive to such an effect. In Sec. V, the static dipolar width of the zero-field relaxation is compared with that of the high-field transverse relaxation. Both an intuitive classical picture and a rigorous quantum mechanical derivation will be presented to obtain the relationship between the two. It is found that the zero-field relaxation function can decay  $(5)^{1/2}$  times faster than the high-field relaxation function due to the contribution of the nonsecular part of the dipolar interaction, which is experimentally demonstrated by observing both  $G_x(t)$  at high field and  $G_z(t)$  at zero field in a  $ZrH_2$  sample. We will discuss the dipolar width in the case of rapid  $\mu^+$  diffusion in Sec. VI, and summary will be given in Sec. VII.

## II. EXPERIMENTAL METHOD

In Fig. 1, a schematic drawing of the longitudinal-field setup is presented. Polarized muon beam is slowed down in a polyethylene degrader, collimated to typically 1.9 cm in diameter and stopped in the

## COUNTER SYSTEM

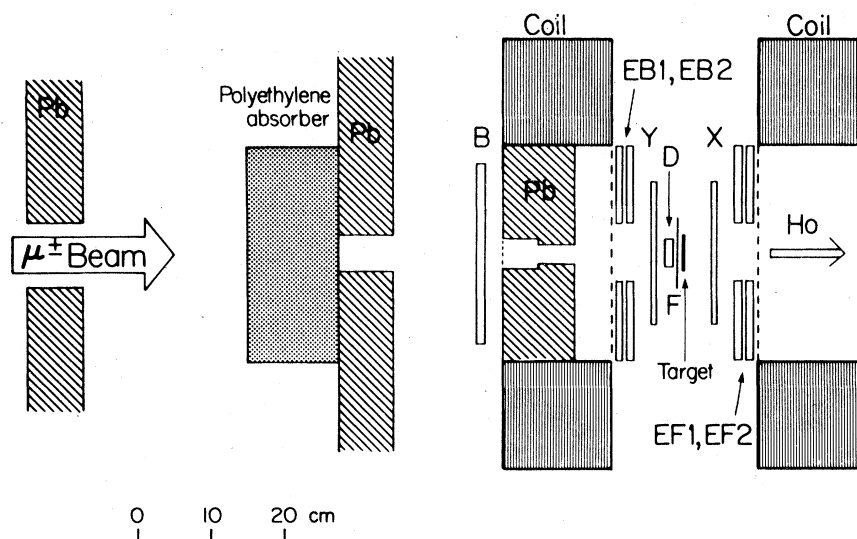


FIG. 1. Schematic drawing of the longitudinal-field setup.

sample placed at the center of the longitudinal coils as shown in the figure. Two sets of positron telescopes are placed at  $0^\circ$  (EB1,EB2) and at  $180^\circ$  (EF1,EF2) to the beam to detect  $\mu - e$  decay positrons. Each counter is square in shape ( $30 \times 30 \text{ cm}^2$ ), and has a 7.5 cm round hole in the center so that it does not see the muon beam directly. Two time spectra, one for each telescope, are accumulated. Since the angular distribution of decay positrons is expressed by Eq. (2),  $G_z(t)$  is obtained by taking the time-differential ratio of two spectra

$$AG_z(t) = \frac{N_z(0,t) - \alpha N_z(\pi,t)}{N_z(0,t) + \alpha N_z(\pi,t)} \quad (3)$$

after proper background subtraction. The instrumental forward/backward asymmetry  $\alpha$  is usually close to 1 in this setup. In many cases,  $\alpha$  can be determined self-consistently by fitting the data, when the relaxation time is definitely shorter than the observation time window, 0–16  $\mu\text{sec}$ . This simple method has been proven to be quite powerful in studying the spin-lattice relaxation time ( $T_1$ ) of the  $\mu^+$  spin in magnetic substances.<sup>2-4</sup> This method is readily applicable to the studies of zero- and low-field relaxation phenomena.

### III. RELAXATION DUE TO STATIC NUCLEAR DIPOLAR FIELDS— $\mu^+$ IN MnSi

As a typical example, we measured  $G_z(t)$  of the  $\mu^+$  in MnSi at room temperature for longitudinal fields of 0, 10, and 30 Oe, as shown in Fig. 2. From the figure, we note the characteristic feature of the zero-

field relaxation function;  $G_z(t)$  at zero field initially shows a Gaussian-like decay, but is followed by a recovery of asymmetry to  $\frac{1}{3}$ . According to the Kubo-Toyabe theory, this recovery of asymmetry to  $\frac{1}{3}$  is an unmistakable evidence for the static character of random fields. In other words, the  $\mu^+$  is definitely

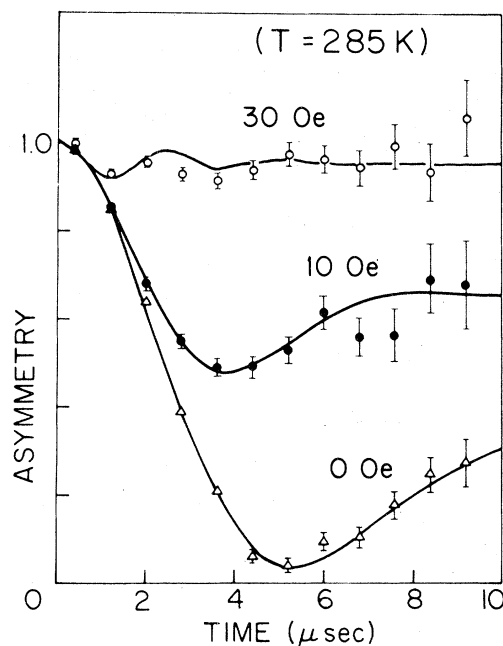


FIG. 2. Observed  $\mu^+$  longitudinal relaxation functions in MnSi at room temperature with 0, 10, and 30 Oe external fields. The solid curves are the best fits to Eq. (10).

frozen at a site, thus seeing static nuclear dipolar fields. This point will be made clear in the following.

Let us first assume that the field  $\vec{H} = (H_x, H_y, H_z)$  is static at each muon site. If a muon stops at  $t = 0$  with its spin pointing to the  $z$  direction, the  $z$  component of the muon spin evolves with time as

$$\sigma_z(t) = \frac{H_z^2}{H^2} + \frac{H_x^2 + H_y^2}{H^2} \cos(\gamma_\mu H t) , \quad (4a)$$

$$= \cos^2\theta + \sin^2\theta \cos(\gamma_\mu H t) , \quad (4b)$$

where  $\theta$  is the polar angle of  $\vec{H}$ . Throughout this paper, we take the  $z$  axis along the external field direction. The zero-field case will be treated as a special case of the longitudinal-field configuration.

We further assume that the random fields are isotropic and each component can be represented by a Gaussian distribution function,

$$P(H_i) = \frac{\gamma_\mu}{(2\pi)^{1/2}\Delta} \exp\left[-\frac{\gamma_\mu^2 H_i^2}{2\Delta^2}\right] \quad (i = x, y, z) , \quad (5)$$

where  $\Delta^2/\gamma_\mu^2$  represents the second moment,

$$\Delta^2/\gamma_\mu^2 = \langle H_x^2 \rangle = \langle H_y^2 \rangle = \langle H_z^2 \rangle . \quad (6)$$

The relaxation function  $G_z(t)$  we observe is just the statistical average of  $\sigma_z(t)$ ;

$$G_z(t) = \int \int \int \sigma_z(t) P(H_x) P(H_y) P(H_z) \\ \times dH_x dH_y dH_z \equiv g_z(t) , \quad (7)$$

which yields

$$g_z(t) = \frac{1}{3} + \frac{2}{3}(1 - \Delta^2 t^2) \exp(-\frac{1}{2}\Delta^2 t^2) . \quad (8)$$

When a longitudinal external field  $\vec{H}_0$  is applied along the  $z$  axis, we simply replace  $P(H_z)$  in Eq. (7) with

$$P(H_z) = \frac{\gamma_\mu}{(2\pi)^{1/2}\Delta} \exp\left[-\frac{\gamma_\mu^2 (H_z - H_0)^2}{2\Delta^2}\right] , \quad (9)$$

and take the statistical average to obtain

$$g_z(t) = 1 - \frac{2\Delta^2}{\omega_0^2} [1 - \exp(-\frac{1}{2}\Delta^2 t^2) \cos\omega_0 t] \\ + \frac{2\Delta^4}{\omega_0^3} \int_0^t \exp(-\frac{1}{2}\Delta^2 \tau^2) \sin\omega_0 \tau d\tau , \quad (10)$$

where  $\omega_0 = \gamma_\mu H_0$ .

The solid curves in Fig. 2 represent best fits of data points to the static Kubo-Toyabe functions, Eq. (10). All the curves are consistently fitted with a single value of  $\Delta/\gamma_\mu = 3.80 \pm 0.04$  Oe. At this temperature, the spin-lattice relaxation time of the  $\mu^+$  spin due to the electron spin fluctuations is known to be longer than 100  $\mu\text{sec}$ .<sup>3</sup> Thus, the relaxation is entirely caused by the random fields from surrounding nuclear dipoles. These random fields are regarded as

static because the relaxation time of nuclear spins is known from NMR to be  $35 \pm 5 \mu\text{sec}$ ,<sup>5</sup> which is much longer than the  $\mu^+$  lifetime.

The zero-field relaxation function Eq. (8) initially shows a Gaussian-like decay, which can be approximated by

$$G_z(t) \sim \exp(-\Delta^2 t^2) \\ = \exp[-\frac{1}{2}(\langle H_x^2 \rangle + \langle H_y^2 \rangle) \gamma_\mu^2 t^2] , \quad (11)$$

where we explicitly indicated that two components of random fields,  $H_x$  and  $H_y$ , contribute to  $G_z(t)$ . On the other hand, the high-field transverse relaxation function in the static limit takes the form (see Sec. IV)

$$G_x(t) = \exp(-\frac{1}{2}\Delta^2 t^2) \\ = \exp(-\frac{1}{2}\langle H_z^2 \rangle \gamma_\mu^2 t^2) , \quad (12)$$

to which only one component of random fields, the component along  $\vec{H}_0$ , contributes. Therefore,  $G_z(t)$  at zero field damps faster than  $G_x(t)$  at high field. Note that  $\frac{1}{2}(\langle H_x^2 \rangle + \langle H_y^2 \rangle)$  at zero field is, in general, not equal to  $\langle H_z^2 \rangle$  at high field; the difference of the width may not be just  $(2)^{1/2}$  but can be as large as  $(5)^{1/2}$ . See Sec. V for details. In view of the fact that  $\mu^+$  lives only for 2.2  $\mu\text{sec}$  while the relaxation time due to nuclear dipolar fields is usually longer than the  $\mu^+$  lifetime, this effective reduction in the time scale should be quite advantageous from experimental viewpoint; the nuclear dipolar width can be determined with better statistical accuracy by using  $G_z(t)$ .

The recovery of asymmetry to  $\frac{1}{3}$  in the zero-field case can be intuitively understood from Eq. (4b); the projection of  $\vec{\sigma}(t)$  on the  $z$  axis averages to  $\frac{1}{3}$ . In a finite longitudinal field, the asymptotic value of the recovery is found to be

$$g_z(\infty) = 1 - \frac{2\Delta^2}{\omega_0^2} + \frac{2\Delta^3}{\omega_0^3} \exp\left[-\frac{\omega_0^2}{2\Delta^2}\right] \\ \times \int_0^{\omega_0/\Delta} \exp(\frac{1}{2}u^2) du , \quad (13)$$

which is larger than  $\frac{1}{3}$  and approaches 1 for large value of  $\omega_0$ .

#### IV. EFFECT OF MUON DIFFUSION

Let us now turn to a more general case by taking the muon diffusion into account, and show that the recovery of  $G_z(t)$  to  $\frac{1}{3}$  is significantly suppressed even in the case of extremely slow muon diffusion.

In the paper of Kubo and Toyabe, the modulation of the field is assumed to follow a Gaussian-

Markovian process. Namely, the correlation of the fluctuating field is characterized by the automoment,

$$\langle H_i(t + \tau) H_i(\tau) \rangle = \Delta^2 / \gamma_\mu^2 \exp(-\nu t) , \quad (14)$$

where  $\tau \equiv 1/\nu$  is the correlation time of the field fluctuation, and the process is described by a diffusion equation of Fokker-Planck type.<sup>6</sup> This implies that the cumulative effect of a large number of random processes contributes to the fluctuation of the local field.

In the present case, however, the process may be better described by a "strong-collision" model.<sup>7</sup> When a muon jumps from site to site with a mean hopping frequency  $\nu$ , the muon experiences a sudden change in the local field, not a gradual change as is described by the Fokker-Planck equation. We idealize this situation by the strong-collision model in which there is no correlation between the fields before and after the jump. The process described by this model is still Markovian, but not Gaussian-Markovian.

#### A. Exact solution of $G_z(t)$ for an arbitrary muon hopping frequency

In this strong-collision model, the time evolution of  $G_z(t)$  consists of contributions from muons which did not jump until time  $t$  [ $g_z^{(0)}(t)$ ], which underwent 1 jump [ $g_z^{(1)}(t)$ ], 2 jumps [ $g_z^{(2)}(t)$ ], etc.,

$$G_z(t) = \sum_{n=0}^{\infty} g_z^{(n)}(t) . \quad (15)$$

It can be easily understood that

$$g_z^{(0)}(t) = e^{-\nu t} g_z(t) , \quad (16)$$

where  $e^{-\nu t}$  is the probability that the muon did not hop until time  $t$ , and  $g_z(t)$  is the static longitudinal relaxation function, Eq. (10). The next term is obtained in the same manner,

$$g_z^{(1)}(t) = \nu \int_0^{\infty} dt_1 e^{-\nu(t-t_1)} g_z(t-t_1) e^{-\nu t_1} g_z(t_1) , \quad (17)$$

which describes the process that the muon experienced a jump at time  $t_1$  ( $0 < t_1 < t$ ). Higher-order terms can be successively derived, and we arrive at the exact expression,

$$F_z(s) = \sum_{n=0}^{\infty} \nu^n f_z^{n+1}(s + \nu) = \frac{f_z(s + \nu)}{1 - \nu f_z(s + \nu)} , \quad (18)$$

where we introduced the Laplace transforms

$$f_z(s) \equiv \int_0^{\infty} g_z(t) e^{-st} dt$$

and

$$F_z(s) \equiv \int_0^{\infty} G_z(t) e^{-st} dt . \quad (19)$$

In Sec. IV C, the same, but more general expressions are derived by using a different formulation, where we show that the transverse relaxation function is also expressed by the same form as Eq. (18).

In the zero-field case,  $f_z(s)$  can be expressed as

$$f_z(s) = \frac{1}{3s} + \frac{2s}{3\Delta^2} \times \left( 1 - s \int_0^{\infty} \exp\left(-\frac{1}{2}\Delta^2 t^2 - st\right) dt \right) . \quad (20)$$

Given this form, it is a straightforward numerical calculation to obtain  $G_z(t)$ , which are presented for several values of  $\tau$  in Fig. 3(a). They are nearly the same as the curves shown in the paper of Kubo and Toyabe. A closer look at the two graphs, however, reveals that the "strong-collision" curves, Fig. 3(a), decay a little slower than the Kubo-Toyabe curves based on the Gaussian-Markovian assumption. The difference is especially notable for the slow hopping ( $\tau\Delta > 1$ ) cases.

For slow hopping, the recovery of asymmetry to  $\frac{1}{3}$  is suppressed and  $G_z(t)$  shows a hump around  $t \sim 3/\Delta$ . The asymptotic form of  $G_z(t)$  may be evaluated by using Eqs. (18) and (20) to be

$$G_z(t) \sim \frac{1}{3} \exp\left(-\frac{2}{3}\nu t\right) \quad (\text{for } t \gg 3/\Delta) , \quad (21)$$

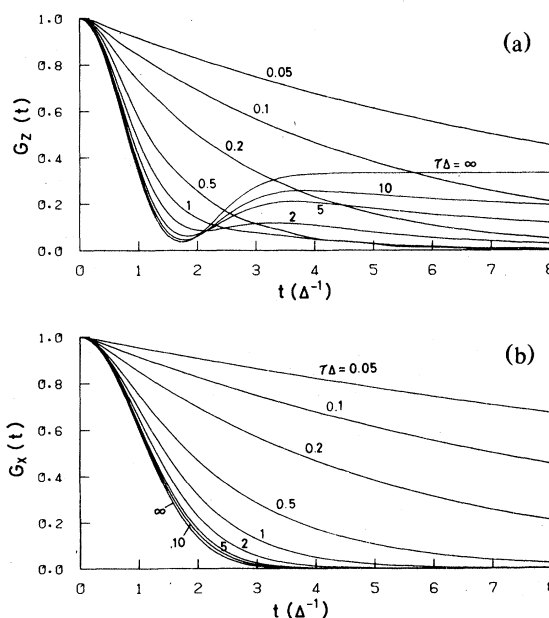


FIG. 3(a). Zero-field longitudinal relaxation functions for different correlation times, numerically calculated from Eq. (18). (b) High-field transverse relaxation function Eq. (22) plotted for different values of  $\tau$  for comparison.

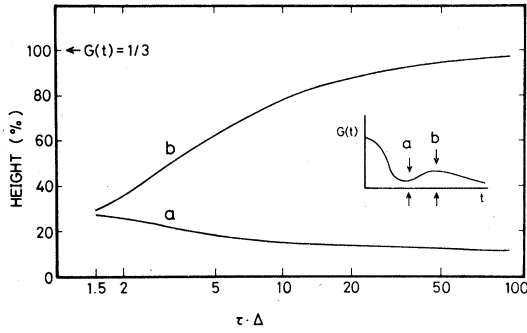


FIG. 4. Height of minimum (a) and hump (b) of the zero-field relaxation function plotted against correlation time  $\tau$ .

where the factor  $\frac{2}{3}$  can be understood intuitively if we note that  $\frac{1}{3}$  of each jump should still preserve the longitudinal polarization. The height of hump provides a very sensitive measure of the correlation time, while the shape in the  $t \leq 2/\Delta$  region is essentially unaltered. This is a very unique feature of the zero-field method. In Fig. 4 we show the dependence of the height of this hump on the hopping time.

By comparing curves in Fig. 3(a) with the zero-field data in MnSi (Fig. 2), we can safely say that the muon diffusion should be slower than  $\tau \sim 5/\Delta$ , or  $\tau > 15 \mu\text{sec}$ , which is much longer than the  $\mu^+$  lifetime. This is the reason we conclude that the  $\mu^+$  is frozen at a site in MnSi even at room temperature.

As the temperature is lowered, both the  $T_1$  of  $^{55}\text{Mn}$  (Ref. 5) and that of  $\mu^+$  (Ref. 3) become shorter. At  $T = 40 \text{ K}$ , for instance, the  $T_1$  of  $^{55}\text{Mn}$  due to the electron-spin fluctuations is estimated to be  $10 \mu\text{sec}$ , while that of  $\mu^+$  is still much longer than its lifetime, around  $40 \mu\text{sec}$ . Then, the nuclear dipolar field felt by the muon is no longer static, and the zero-field relaxation function  $G_z(t)$  should indicate slow modulation around  $\tau\Delta \sim 3$ . This suggests an interesting possibility of measuring the nuclear zero-field spin-lattice relaxation time, indirectly from the muon zero-field relaxation function.

#### B. Comparison with the high-field transverse relaxation

For comparison, we also plotted transverse relaxation functions  $G_x(t)$  for high field in Fig. 3(b), which takes the form<sup>8</sup>

$$G_x(t) = \exp[-\Delta^2 \tau^2 (e^{-t/\tau} - 1 + t/\tau)] \quad (22)$$

As is evident from Fig. 3(b), it is impossible to ex-

tract information on slow modulation ( $\tau\Delta \geq 1$ ) from the observation of  $G_x(t)$  in the conventional precession measurement. Therefore, the zero-field method is powerful for studies of diffusion/trapping of  $\mu^+$ .

As is well known, the expression Eq. (22) is derived based on the Gaussian-Markovian assumption. The strong-collision model for the high-field transverse relaxation leads to an expression similar to Eq. (18) [see Eq. (34)], whose inverse transform was numerically performed and was carefully compared with the curve of Eq. (22) by Kehr *et al.*<sup>9</sup> Just like our result for  $G_z(t)$ , the strong-collision model was shown to lead to a slower damping of  $G_x(t)$ . However, the difference is small so that the simple analytic expression Eq. (22) is preferred for data analysis over Eq. (18).

#### C. Alternative method to solve the strong-collision model

Here, we present an alternative method to solve the strong-collision model which uses the distribution function  $P(\vec{M}, \vec{H}, t)$ , the probability density of spin  $\vec{M}$  and the random field  $\vec{H}$  at a given time  $t$ . The function  $P(\vec{M}, \vec{H}, t)$  follows the equation<sup>10</sup>

$$\begin{aligned} \frac{\partial}{\partial t} P(\vec{M}, \vec{H}, t) = & -\gamma \vec{M} \times \vec{H} \cdot \frac{\partial}{\partial \vec{M}} P(\vec{M}, \vec{H}, t) \\ & - \int P(\vec{M}, \vec{H}, t) w(\vec{H} \rightarrow \vec{H}') d\vec{H}' \\ & + \int P(\vec{M}, \vec{H}', t) w(\vec{H}' \rightarrow \vec{H}) d\vec{H}', \end{aligned} \quad (23)$$

where the first term represents the precession of  $\vec{M}$  in the field  $\vec{H}$  and the latter two terms describe the random modulation of the local field.

The "strong-collision" assumption means that a sudden change of the local field leads immediately to the equilibrium probability distribution  $P_0(\vec{H})$ , i.e.,

$$w(\vec{H}' \rightarrow \vec{H}) = \nu P_0(\vec{H}), \quad (24)$$

independent of  $\vec{H}'$ . Under this assumption, Eq. (23) is simplified to

$$\begin{aligned} \frac{\partial}{\partial t} P(\vec{M}, \vec{H}, t) = & -\gamma \vec{M} \times \vec{H} \cdot \frac{\partial}{\partial \vec{M}} P(\vec{M}, \vec{H}, t) \\ & - \nu P(\vec{M}, \vec{H}, t) \\ & + \nu P_0(\vec{H}) \int P(\vec{M}, \vec{H}', t) d\vec{H}', \end{aligned} \quad (25)$$

with the initial condition

$$P(\vec{M}, \vec{H}, 0) = \delta(\vec{M} - \vec{M}_0) P_0(\vec{H}) \quad (26)$$

We introduce here the vector function

$$\mathfrak{M}(\vec{H}, s) = \int_0^\infty dt e^{-st} \int \vec{M} P(\vec{M}, \vec{H}, t) d\vec{M}, \quad (27)$$

and its average

$$\overline{\mathfrak{M}}(s) = \int \mathfrak{M}(\vec{H}, s) d\vec{H}, \quad (28)$$

$$\mathfrak{M}(\vec{H}, s) = \frac{P_0(\vec{H})}{u(u^2 + \omega^2)} \begin{bmatrix} u^2 + \omega_x^2 & \omega_z u + \omega_x \omega_y & -\omega_y u + \omega_x \omega_z \\ -\omega_z u + \omega_y \omega_x & u^2 + \omega_y^2 & \omega_x u + \omega_y \omega_z \\ \omega_y u + \omega_z \omega_x & -\omega_x u + \omega_z \omega_y & u^2 + \omega_z^2 \end{bmatrix} [\nu \overline{\mathfrak{M}}(s) + \vec{M}_0]. \quad (30)$$

We assume that the field  $\vec{H}$  is cylindrically symmetric around the  $z$  axis, and integrate the both sides of Eq. (30) with respect to  $\vec{H}$  to obtain

$$\overline{\mathfrak{M}}(s) = \begin{bmatrix} f_1'(u) & f_1''(u) & 0 \\ -f_1''(u) & f_1'(u) & 0 \\ 0 & 0 & f_{||}(u) \end{bmatrix} (\nu \overline{\mathfrak{M}}(s) + \vec{M}_0), \quad (31)$$

where  $f_1'$ ,  $f_1''$ , and  $f_{||}$  are defined as

$$f_1'(u) = \left\langle \frac{u^2 + \omega_x^2}{u(u^2 + \omega^2)} \right\rangle, \quad f_1''(u) = \left\langle \frac{\omega_z}{u^2 + \omega^2} \right\rangle$$

and

$$f_{||}(u) = \left\langle \frac{u^2 + \omega_z^2}{u(u^2 + \omega^2)} \right\rangle. \quad (32)$$

The brackets mean averaging over the distribution  $P_0(\vec{H})$ . Finally, the expression describing the longitudinal relaxation becomes

$$\mathfrak{M}_z(s) = \frac{f_{||}(s + \nu)}{1 - \nu f_{||}(s + \nu)} M_{0z}. \quad (33)$$

We also obtain

$$\mathfrak{M}_+(s) = \frac{f_{+-}(s + \nu)}{1 - \nu f_{+-}(s + \nu)} M_{0+} \quad (34)$$

$$(M_+ = M_x + iM_y, \quad f_{+-} = f_1' - if_1'')$$

which describes the transverse relaxation. Equations (33) and (34) are equivalent to Eq. (18) derived in a different formulation.

## V. NUCLEAR DIPOLAR BROADENING AT ZERO FIELD

### A. Classical picture

Here, we raise a question: what is  $\Delta^2$ ? For the conventional transverse-field method, where the applied field is large enough compared with the nuclear

for which Eqs. (25) and (26) give the equation

$$s\mathfrak{M}(\vec{H}, s) = -\gamma \vec{H} \times \mathfrak{M}(\vec{H}, s) - \nu \mathfrak{M}(\vec{H}, s) + P_0(\vec{H}) [\nu \overline{\mathfrak{M}}(s) + \vec{M}_0]. \quad (29)$$

By using the notation  $\gamma H_0 \equiv (\omega_x, \omega_y, \omega_z)$  and  $u \equiv s + \nu$ , we can solve Eq. (29) with respect to  $\mathfrak{M}(\vec{H}, s)$ ;

dipolar fields, we take the second moment à la Van Vleck  $\sigma_{VV}^2$ .<sup>11,12</sup> However, much precaution should be paid for the present case of zero- and low-field relaxation. In order to clarify the point, an intuitive argument may be helpful.

The nuclear dipolar field at origin from an  $i$ th point dipole  $\vec{\mu}_i$  located at  $\vec{r}_i$  is

$$\vec{H}_i = \frac{\mu_i}{r_i^3} [3(\hat{\mu}_i \cdot \hat{r}_i)\hat{r}_i - \hat{\mu}_i]. \quad (35)$$

Its  $z$  component can be expressed as

$$H_{iz} = \frac{\mu_i}{r_i^3} [(3 \cos^2 \Theta_i - 1) \cos \theta_i + 3 \sin \Theta_i \cos \Theta_i \sin \theta_i \cos \phi_i], \quad (36)$$

where  $\Theta_i$  is polar angle of  $\vec{r}_i$ ,  $\theta_i$  is polar angle of  $\vec{\mu}_i$ , and  $\phi_i$  is azimuth angle of  $\vec{\mu}_i$ . In the transverse-field case, where the nuclear Larmor frequency  $\gamma_i H_0$  is larger than the width due to random field  $\gamma_\mu H_i$ , namely,

$$H_0 \gg (\gamma_\mu / \gamma_i) H_i, \quad (37)$$

the Larmor precession of  $\vec{\mu}_i$  around  $\vec{H}_0 \parallel z$  averages out the second term (nonsecular part) in Eq. (36); the mean-square value of the secular component along  $\vec{H}_0$  reduces to the Van Vleck value,

$$\sigma_{VV}^2 = \frac{1}{3} \sum_i B_i (3 \cos^2 \Theta_i - 1)^2, \quad (38)$$

where

$$B_i \equiv I(I+1) \gamma_\mu^2 \gamma_i^2 \hbar^2 r_i^{-6}. \quad (39)$$

Its polycrystalline average is

$$\overline{\sigma_{VV}^2} = \frac{4}{15} \sum_i B_i. \quad (40)$$

Even at zero field, the surrounding nuclei may be precessing due to the electric quadrupole (eqQ) interaction. If the eqQ precession frequency  $\omega_Q$  is larger than  $\gamma_\mu H_i$ , the field-averaging similar to the high-field precession case should result. If we denote

the unit vector of the electric-field-gradient direction at  $i$ th nucleus by  $\hat{q}_i$ , the mean-square value of the component along the muon spin direction can be expressed as

$$\begin{aligned} (\sigma_{QI}^2)_z &= \sum_i \gamma_\mu^2 H_{iz}^2 \\ &= \frac{1}{3} \sum_i B_i [3(\hat{q}_i \cdot \hat{r}_i) \cos \Theta_i - \hat{q}_{iz}]^2, \end{aligned} \quad (41)$$

where  $\Theta_i$  in the zero-field case is defined as the polar angle of  $\hat{r}_i$  with respect to the initial muon spin direction. Hartmann<sup>13</sup> pointed out that the presence of the interstitial  $\mu^+$  creates a radially directed electric field gradient on surrounding nuclei, which can affect the width of the high-field transverse precession signal; it was experimentally verified by Camani *et al.*<sup>14</sup> for the case of  $\mu^+$  in copper. When there is no external field, the nuclear quantization axis  $\hat{q}_i$  is each radial direction  $\hat{r}_i$ , so that

$$(\sigma_{QI}^2)_x + (\sigma_{QI}^2)_y = \frac{4}{3} \sum_i^{nn} B_i \sin^2 \Theta_i, \quad (42)$$

and its polycrystalline average is

$$(\bar{\sigma}_{QI}^2)_x + (\bar{\sigma}_{QI}^2)_y = \frac{8}{9} \sum_i^{nn} B_i \quad (43)$$

(however, see note added in proof).

If eqQ is not so strong, or when  $I = \frac{1}{2}$ , the nonsecular term does not drop out any more and the  $\mu^+$  spin feels the full magnitude of  $\bar{\mu}_i$ . From Eq. (35), we obtain the mean-square value of the full magnitude of  $\bar{\mu}_i$  to be

$$\sum_i \gamma_\mu^2 \bar{\mu}_i^2 = 2 \sum_i B_i \equiv \sigma_i^2, \quad (44)$$

while the mean-square value of the  $z$  component becomes

$$\sum_i \gamma_\mu^2 H_{iz}^2 = \frac{1}{3} \sum_i B_i (3 \cos^2 \Theta_i + 1) \equiv (\sigma_{ZF}^2)_z. \quad (45)$$

Similarly, the components responsible for the longitudinal relaxation are obtained as

$$(\sigma_{ZF}^2)_x + (\sigma_{ZF}^2)_y = \frac{1}{3} \sum_i B_i (5 - 3 \cos^2 \Theta_i). \quad (46)$$

As expected, we find that Eqs. (45) and (46) add up to

$$(\sigma_{ZF}^2)_x + (\sigma_{ZF}^2)_y + (\sigma_{ZF}^2)_z = \sigma_i^2. \quad (47)$$

If we take the polycrystalline average, or if the muon site has a cubic symmetry (note that  $\langle \cos^2 \theta \rangle = \frac{1}{3}$  in either case), we obtain

$$\bar{\sigma}_{ZF}^2 = \frac{2}{3} \sum_i B_i = \frac{1}{3} \sigma_i^2 = \frac{5}{2} \bar{\sigma}_{VV}^2, \quad (48)$$

which is  $\frac{5}{2}$  times larger than  $\bar{\sigma}_{VV}^2$ . If this is the case,

the width of the zero-field relaxation function [which picks up another factor  $(2)^{1/2}$  since two components of random fields contribute] and that of the high-field transverse relaxation function should differ by a factor  $(5)^{1/2}$ . It will be shown in Sec. VC that the classical argument presented here gives the same correct answer as the quantum-mechanical treatment.

### B. Experimental comparison of $G_z(t)$ and $G_x(t) - \mu^+$ in ZrH<sub>2</sub>

To examine the relation predicted by Eq. (48), we chose ZrH<sub>2</sub> (polycrystal) as a sample, and measured both  $G_z(t)$  at zero field and  $G_x(t)$  at high field. ZrH<sub>2</sub> is ideally suited for this purpose since no eqQ interaction is present, the dipolar field created by protons is conveniently large and the  $\mu^+$  is known to diffuse very slowly in ZrH<sub>2</sub> from a zero-field experiment by Doyama *et al.*<sup>15</sup> In Fig. 5, the observed  $G_z(t)$  and  $G_x(t)$  are plotted. At room temperature, the zero-field measurement yielded a curve similar to the case of MnSi (though it indicated a slow modulation  $\tau\Delta = 3.5 \pm 1.0$ ), and  $\bar{\sigma}_{ZF}$  was determined to be  $0.514 \pm 0.008/\mu\text{sec}$ . In a transverse field of 5.0 kOe,  $G_x(t)$  yielded  $\bar{\sigma}_{VV} = 0.329 \pm 0.006/\mu\text{sec}$ . Thus, we obtain the ratio

$$\bar{\sigma}_{ZF}^2 / \bar{\sigma}_{VV}^2 = 2.4 \pm 0.1,$$

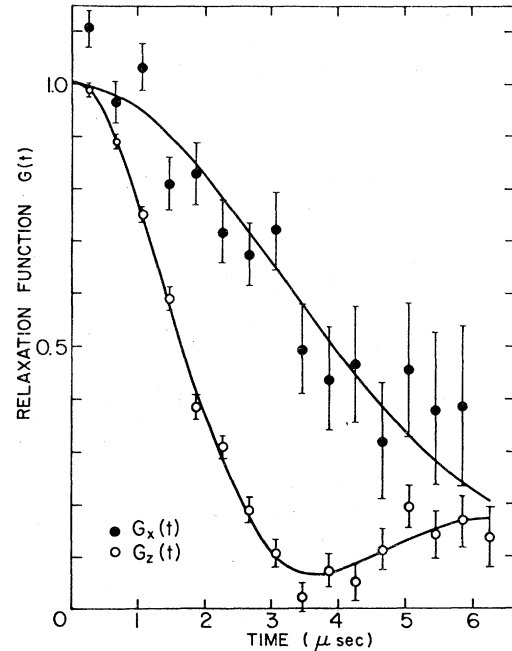


FIG. 5. Observed zero-field relaxation function  $G_z(t)$  and high-field transverse relaxation function  $G_x(t)$  in ZrH<sub>2</sub> at room temperature.

in good agreement with the factor  $\frac{5}{2}$ , presented in Eq. (48).

The zero-field dipolar broadening parameters were calculated according to Eq. (48), for two different muon sites. Assuming that the muon occupies a proton site, the calculation yielded  $\Delta(H) = 0.335/\mu\text{sec}$ . If we assume that the muon is at an interstitial site (octahedral site with respect to the surrounding Zr nuclei), we obtained  $\Delta(IS) = 0.557/\mu\text{sec}$ . Therefore, the observed value  $\bar{\sigma}_{ZF} = 0.514/\mu\text{sec}$  indicates that the muon occupies the interstitial site, possibly inducing a slight local lattice expansion.<sup>14</sup> This does not exclude the possibility that some of the muons occupy proton sites, however.

We also would like to point out that the experimental fit which gives  $\tau\Delta = 3.5 \pm 1.0$  can be reasonably explained by attributing  $\tau$  to proton-proton dipolar coupling. We take account of the fact that the second moment for like spins (proton-proton) is  $\frac{3}{2}$  times larger than that for unlike spins (muon-proton) at zero field, and assume that the muon is at an interstitial site as mentioned above. Then, we obtain

$$\tau\Delta = [\Delta(IS)/\Delta(H)] \times (\frac{2}{3})^{1/2} \times (\gamma_\mu/\gamma_p) = 4.3 ,$$

which agrees fairly well with the experimental value.

### C. Quantum-mechanical treatment

Here, we apply the general quantum-mechanical theory of magnetic resonance linewidth formulated by Kubo and Tomita<sup>8</sup> to derive some of the useful expressions for the muon spin relaxation, and also to show that the classical argument presented in Sec. V A yields correct answers.

We write the effective Hamiltonian for the muon spin  $\bar{S}$  in the form

$$\mathcal{H} = -\gamma_\mu \hbar S_z H_0 + \mathcal{H}_d , \quad (49)$$

where  $\mathcal{H}_d$  represents the dipolar interaction,

$$\mathcal{H}_d = \sum_i \gamma_\mu^2 \gamma^2 \hbar^2 [(\bar{S} \cdot \bar{I}_i) r_i^{-2} - 3(\bar{S} \cdot \bar{r}_i)(\bar{I}_i \cdot \bar{r}_i)] / r_i^5 . \quad (50)$$

Using the perturbation method following Kubo-Tomita's procedure, the relaxation functions can be approximately given by the expressions

$$G_z(t) = \exp[\psi_z(t)] , \quad (51a)$$

$$\begin{aligned} \psi_z(t) = & -\sum_i B_i \left[ \frac{1}{6} (3 \cos^2 \Theta_i - 1)^2 g_\nu(\omega_\mu - \omega_i, t) \right. \\ & + 3 \sin^2 \Theta_i \cos^2 \Theta_i g_\nu(\omega_\mu, t) \\ & \left. + \frac{3}{2} \sin^4 \Theta_i g_\nu(\omega_\mu + \omega_i, t) \right] , \quad (51b) \end{aligned}$$

$$G_x(t) = \exp[\psi_x(t)] , \quad (52a)$$

$$\begin{aligned} \psi_x(t) = & -\sum_i B_i \left[ \frac{1}{3} (3 \cos^2 \Theta_i - 1)^2 g_\nu(0, t) \right. \\ & + 3 \sin^2 \Theta_i \cos^2 \Theta_i g_\nu(\omega_i, t) \\ & \left. + \frac{1}{2} \psi_z(t) \right] , \quad (52b) \end{aligned}$$

where  $\omega_\mu \equiv \gamma_\mu H_0$ ,  $\omega_i \equiv \gamma_i H_0$ , and

$$g_\nu(\omega, t) \equiv \int_0^t (t - \tau) f_\nu(\tau) \cos \omega \tau d\tau . \quad (53)$$

To proceed further, we assume that the correlation function  $f_\nu(t)$  takes the form

$$f_\nu(t) = \exp(-\nu|t|) . \quad (54)$$

Then,

$$g_\nu(\omega, t) = \text{Re} \left[ \frac{e^{-\nu t} e^{i\omega t} - 1 + (\nu - i\omega)t}{(\nu - i\omega)^2} \right] , \quad (55)$$

whose asymptotic behaviors for the static and the narrowing limits are

$$g_{\nu \rightarrow 0}(\omega, t) \rightarrow (1 - \cos \omega t) / \omega^2 , \quad (56a)$$

$$g_{\nu \rightarrow \infty}(\omega, t) \rightarrow \frac{t}{\nu(\omega^2 + \nu^2)} = \frac{\tau t}{1 + \omega^2 \tau^2} . \quad (56b)$$

For simplicity, let us take the polycrystalline averages of Eqs. (51) and (52);

$$\begin{aligned} \bar{\psi}_z(t) = & -\bar{\sigma}_{\nu\nu}^2 \left[ \frac{1}{2} g_\nu(\omega_\mu - \omega_i, t) + \frac{3}{2} g_\nu(\omega_\mu, t) \right. \\ & \left. + 3 g_\nu(\omega_\mu + \omega_i, t) \right] , \quad (57) \end{aligned}$$

$$\bar{\psi}_x(t) = -\bar{\sigma}_{\nu\nu}^2 [g_\nu(0, t) + g_\nu(\omega_i, t)] + \frac{1}{2} \bar{\psi}_z(t) . \quad (58)$$

The first term in Eq. (58) represents the secular width, while all other terms are due to nonsecular contributions.

In the static limit, we find, from Eqs. (56a) and (58), that  $\omega_i \gg \bar{\sigma}_{\nu\nu}$  needs to be satisfied in order that all the nonsecular contributions become negligible. When this high-field condition is satisfied, the transverse relaxation function in the static limit becomes

$$G_x(t) \rightarrow \exp\left(-\frac{1}{2} \bar{\sigma}_{\nu\nu}^2 t^2\right) . \quad (59)$$

The zero-field longitudinal relaxation function in the static limit, on the other hand, takes the form

$$G_z(t) \rightarrow \exp\left(-\frac{1}{2} 5 \bar{\sigma}_{\nu\nu}^2 t^2\right) . \quad (60)$$

The enhancement factor 5 was already predicted by using the classical argument in Sec. V A.

## VI. DIPOLAR WIDTH IN THE CASE OF RAPID MUON DIFFUSION

Finally, we would like to comment on the relaxation rate in the case of rapid  $\mu^+$  diffusion. When the



hopping time becomes short, or more quantitatively, when the condition  $\tau\sigma \ll 1$  is satisfied, both  $G_z(t)$  and  $G_x(t)$  become exponential;

$$G_z(t) = \exp(-t/T_1) = \exp\left[-\bar{\sigma}_{VV}^2\tau t \left( \frac{1}{2(1+(\omega_\mu - \omega_I)^2\tau^2)} + \frac{3}{2(1+\omega_\mu^2\tau^2)} + \frac{3}{1+(\omega_\mu + \omega_I)^2\tau^2} \right)\right], \quad (61)$$

$$G_x(t) = \exp(-t/T_2) = \exp\left[-\bar{\sigma}_{VV}^2\tau t \left( 1 + \frac{3}{2(1+\omega_I^2\tau^2)} \right) - \frac{t}{2T_1}\right]. \quad (62)$$

When  $\omega_I^{-1} \ll \tau \ll \bar{\sigma}_{VV}^{-1}$ , the high-field relaxation rate takes the familiar form

$$\frac{1}{T_2} = \bar{\sigma}_{VV}^2\tau. \quad (63)$$

When the hopping time becomes shorter than the nuclear Larmor period ( $\omega_I\tau \ll 1$ ), it should look as though the surrounding nuclei are at rest seen from the rapidly diffusing  $\mu^+$ , so that the  $\mu^+$  should instantaneously see the full magnitude of nuclear dipolar fields, not  $\bar{\sigma}_{VV}^2$  but  $\bar{\sigma}_{ZF}^2 = \frac{5}{2}\bar{\sigma}_{VV}^2$ , just like the case of the zero-field relaxation. In this region, Eqs. (61) and (62) yield

$$\frac{1}{T_1} = \frac{5\bar{\sigma}_{VV}^2\tau t}{1+\omega_\mu^2\tau^2}, \quad (64)$$

$$\frac{1}{T_2} = \frac{5}{2}\bar{\sigma}_{VV}^2\tau t \left( 1 + \frac{1}{1+\omega_\mu^2\tau^2} \right). \quad (65)$$

Finally, when  $\tau$  is much shorter than the Larmor period of  $\mu^+$  ( $\omega_\mu\tau \ll 1$ ), the longitudinal relaxation time  $T_1$  becomes equal to the transverse relaxation time  $T_2$ ,

$$\frac{1}{T_1} = \frac{1}{T_2} = 5\bar{\sigma}_{VV}^2\tau. \quad (66)$$

There is a factor 5 difference between Eqs. (63) and (66), which, of course, comes from the nonsecular part of the dipolar interaction. The same situation exists in NMR or in ESR, as was first pointed out by Anderson and Weiss<sup>16</sup> for the case of exchange-narrowed paramagnetic resonance linewidth. The enhancement factor for like-spin systems is  $\frac{10}{3}$ , so that this is usually referred to as the  $\frac{10}{3}$  effect.<sup>8,11</sup>

In Fig. 6, the transverse relaxation rate  $1/T_2$  is plotted against the  $\mu^+$  hopping time, which schematically presents how the nonsecular part of the dipolar interaction enhances the dipolar width as the  $\mu^+$  hopping frequency is increased or, equivalently, as the external field is decreased. We note the characteristic feature of the "5 effect" for  $\mu^+$  not found in the motional narrowing of the NMR linewidth, i.e., the nonsecular part of the dipolar interaction comes into play at two different hopping frequencies. Because  $\gamma_\mu$  and  $\gamma_I$  differ typically by a factor 10, the effect appears as the two distinct shoulders in Fig. 6. An enhance-

ment by a factor  $\frac{5}{2}$  takes place when  $\nu$  exceeds  $\omega_I$ , and the  $\mu^+$  sees the full magnitude of dipolar fields including nonsecular  $x$  and  $y$  components. An enhancement by another factor 2 occurs when  $\nu$  exceeds  $\omega_\mu \sim 10\omega_I$ , where the fluctuating random fields can induce the transition between the muonic Zeeman levels.

This latter process may be best understood in terms of the simple expressions given by the Redfield theory.<sup>17</sup>

$$\frac{1}{T_1} = \gamma_\mu^2\tau \frac{\langle H_x^2 \rangle + \langle H_y^2 \rangle}{1+\omega_\mu^2\tau^2}, \quad (67)$$

$$\frac{1}{T_2} = \gamma_\mu^2\tau \left\{ \langle H_z^2 \rangle + \frac{\langle H_x^2 \rangle + \langle H_y^2 \rangle}{2(1+\omega_\mu^2\tau^2)} \right\}. \quad (68)$$

If we classically evaluate the mean-square values of random fields due to nuclear dipoles when  $\omega_I\tau \ll 1$  [Eqs. (45)–(48)], the above Redfield expressions become equal to Eqs. (64) and (65), derived from the Kubo-Tomita theory. The dependence of  $T_1$  and  $T_2$  on the crystal axis orientation in the narrowing limit, which has been neglected so far, can be easily obtained to be

$$\frac{1}{T_1} \rightarrow \gamma_\mu^2\tau (\langle H_x^2 \rangle + \langle H_y^2 \rangle) = \frac{1}{3}\tau \sum_i B_i(5 - 3\cos^2\Theta_i), \quad (69)$$

$$\frac{1}{T_2} \rightarrow \gamma_\mu^2\tau \langle H_z^2 \rangle + \frac{1}{2T_1} = \frac{1}{6}\tau \sum_i B_i(7 + 3\cos^2\Theta_i). \quad (70)$$

We see that if the  $\mu^+$  hops among sites having cubic

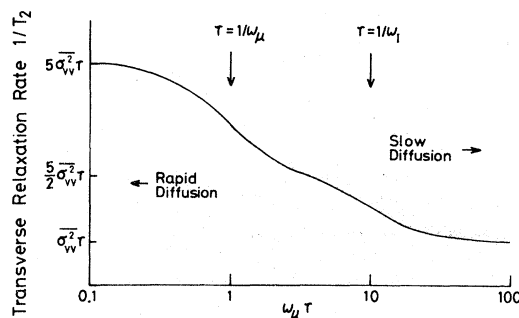


FIG. 6. Transverse relaxation rate  $1/T_2$  is plotted against  $\omega_\mu\tau$ , where we assumed  $\omega_\mu = 10\omega_I$ .

symmetry, neither  $T_1$  nor  $T_2$  will depend on the crystal axis orientation.

We stress that these nonsecular contribution effects should be correctly taken into account when deducing the  $\mu^+$  hopping time from the observed  $\mu^+$  relaxation function.

## VII. CONCLUDING REMARKS

We have shown that the zero-field relaxation function, which is inaccessible to NMR, can be studied easily by using  $\mu^+$ , and that it has many practical advantages over the widely used transverse-field method. In particular, slow modulation of random fields can be studied remarkably well.

The nuclear dipolar width in the zero-field situation has been examined in detail, both theoretically and experimentally, in comparison with the high-field relaxation width. A factor 5 enhancement of the second moment of the zero-field relaxation over the high-field transverse relaxation has been predicted, which was also experimentally demonstrated. Motional narrowing of the muon relaxation function has also been discussed in detail.

*Note added in proof.* Quantum mechanically, Eqs.

(42) and (43) should read

$$(\sigma_{Ql}^2)_x + (\sigma_{Ql}^2)_y = \frac{1}{3} \sum_i^{nn} B_i \left[ 4 \sin^2 \Theta_i + \frac{3(I+1/2)}{4I(I+1)} \times (2 - \sin^2 \Theta_i) \right] \quad (42')$$

and

$$(\bar{\sigma}_{Ql}^2)_x + (\bar{\sigma}_{Ql}^2)_y = \frac{8}{9} \sum_i^{nn} B_i \left[ 1 + \frac{3(I+1/2)}{8I(I+1)} \right], \quad (43')$$

respectively, when the nuclear spin  $I$  is half integer (where nn stands for nearest neighbor). Since the eqQ energies of  $I_z = \pm \frac{1}{2}$  are degenerate, the zero-frequency transitions between  $I_z = \pm \frac{1}{2}$  have to be taken into account to calculate the width.

## ACKNOWLEDGMENTS

The authors are indebted to Professor H. Yasuoka, Professor Y. Ishikawa, and Professor M. Doyama for helpful collaborations. This work was supported by Japan Society for the Promotion of Science, the Toray Science Foundation, the Grant-in-Aid of the Japanese Ministry of Education, Culture and Science, and the Atomic Energy Control Board and NRC.

- 
- <sup>1</sup>R. Kubo and T. Toyabe, in *Magnetic Resonance and Relaxation*, edited by R. Blinc (North-Holland, Amsterdam, 1967), p. 810; T. Toyabe, M.S. thesis (University of Tokyo, 1966) (unpublished).
- <sup>2</sup>R. S. Hayano, Y. J. Uemura, J. Imazato, N. Nishida, K. Nagamine, T. Yamazaki, and H. Yasuoka, *Phys. Rev. Lett.* **41**, 421 (1978).
- <sup>3</sup>R. S. Hayano, Y. J. Uemura, J. Imazato, N. Nishida, T. Yamazaki, H. Yasuoka, and Y. Ishikawa, *Phys. Rev. Lett.* **41**, 1743 (1978).
- <sup>4</sup>T. Yamazaki, *Hyperfine Interactions* **6**, 115 (1979).
- <sup>5</sup>H. Yasuoka, V. Jaccarino, R. C. Sherwood and J. H. Wernick, *J. Phys. Soc. Jpn.* **44**, 842 (1978).
- <sup>6</sup>M. C. Wang and G. E. Uhlenbeck, *Rev. Mod. Phys.* **17**, 323 (1945).
- <sup>7</sup>R. Kubo, *J. Phys. Soc. Jpn.* **9**, 935 (1954).
- <sup>8</sup>R. Kubo and K. Tomita, *J. Phys. Soc. Jpn.* **9**, 888 (1954).
- <sup>9</sup>K. W. Kehr, G. Honig, and D. Richter (unpublished).
- <sup>10</sup>R. Kubo, in *Stochastic Processes in Chemical Physics*, edited by K. Shuler (Wiley, New York, 1969), p. 101.
- <sup>11</sup>J. H. Van Vleck, *Phys. Rev.* **74**, 1168 (1948); *Nuovo Cimento Suppl.* **3**, 993 (1956).
- <sup>12</sup>N. Bloembergen, E. M. Purcell, and R. V. Pound, *Phys. Rev.* **73**, 679 (1948).
- <sup>13</sup>O. Hartmann, *Phys. Rev. Lett.* **39**, 832 (1977).
- <sup>14</sup>M. Camani, F. N. Gyax, W. Rüegg, A. Schenck, and H. Shilling, *Phys. Rev. Lett.* **39**, 836 (1977).
- <sup>15</sup>M. Doyama and R. Nakai (private communication).
- <sup>16</sup>P. W. Anderson and P. R. Weiss, *Rev. Mod. Phys.* **25**, 269 (1953).
- <sup>17</sup>See, for example, C. P. Slichter, *Principles of Magnetic Resonance* (Harper and Row, New York, 1963).